Nature and relationships of *Sahelanthropus tchadensis*

Roberto Macchiarelli [a, b, *], Aude Bergeret-Medina [c], Damiano Marchi [d, e], Bernard Wood [f]

[a] *Unité de Formation Géosciences, Université de Poitiers, 86073 Poitiers, France*

[b] *Département Homme & Environnement, UMR 7194 CNRS, Muséum national d'Histoire naturelle, 75116 Paris, France*

[c] *448C, Chemin de Souilles, 82410 Saint-Etienne-de-Tulmont, France*

[d] *Department of Biology, University of Pisa, 56126 Pisa, Italy*

[e] *Evolutionary Studies Institute and Centre for Excellence in PalaeoSciences, University of the Witwatersrand, Wits 2050, South Africa*

[f] *Center for the Advanced Study of Human Paleobiology and Department of Anthropology, George Washington University, Washington, DC 20052, USA*

* Corresponding author.

E-mail address: roberto.macchiarelli@univ-poitiers.fr (R. Macchiarelli).

Keywords: Hominid; Hominin; *Sahelanthropus tchadensis*; Femur

ABSTRACT

A partial left femur (TM 266-01-063) was recovered in July 2001 at Toros-Menalla, Chad, at the same fossiliferous location as the late Miocene holotype of *Sahelanthropus tchadensis* (the cranium TM 266-01-060-1). It was recognized as a probable primate femur in 2004, when one of the authors was undertaking a taphonomic survey of the fossil assemblages from Toros-Menalla. We are confident the TM 266 femoral shaft belongs to a hominid. It could sample a hominid hitherto unrepresented at Toros-Menalla, but a more parsimonious working hypothesis is that it belongs to *S. tchadensis*. The differences between TM 266 and the late Miocene *Orrorin tugenensis* partial femur BAR 1002'00, from Kenya, are consistent with maintaining at least a species-level distinction between *S. tchadensis* and *O. tugenensis.* The results of our preliminary functional analysis suggest the TM 266 femoral shaft belongs to an individual that was not habitually bipedal, something that should be taken into account when considering the relationships of *S. tchadensis*. The circumstances of its discovery should encourage researchers to check to see whether there is more postcranial evidence of *S. tchadensis* among the fossils recovered from Toros-Menalla.

1. Introduction

There are now several lines of evidence—morphological, molecular and genetic—to support the hypothesis that the living taxa most closely related to modern humans are chimpanzees and bonobos (Ruvolo, 1997; Prado-Martinez et al., 2013; Diogo et al., 2017). Most attempts to calibrate the DNA differences suggest the human (hominin) lineage has been separate from the *Pan* (panin) lineage for ca. 8–6 Myr (Bradley, 2008; Stone et al., 2010), but extrapolations based on generation times in *Pan* and *Gorilla* (Langergraber et al., 2012; see also Moorjani et al., 2016) suggest the divergence date may be earlier. Two putative hominin taxa are known from ca. 8–6 Ma in Africa. One, *Orrorin tugenensis*, was established to accommodate dental and postcranial remains recovered from ca. 6.0 Ma Lukeino Formation sediments exposed at Aragai, Cheboit, Kapcheberek and Kapsomin in the Baringo District, Kenya (Senut et al., 2001). This contribution focuses on the other taxon, *Sahelanthropus tchadensis*, which was established to accommodate fossil remains from Chad (Brunet et al., 2002).

The first published evidence for *S. tchadensis* consisted of six fossils—including the holotype specimen, an adult cranium (TM 266-01-060-1, hereafter the TM 266 cranium)—all of which were recovered from a single locality, TM 266, in the informal 'anthracotheriid unit' at Toros-Menalla (Brunet et al., 2002). Additional specimens recovered in 2001 and 2002, including an upper premolar tooth from TM 266, and two mandibles, TM 247-01-02 and TM 292-02-01 (Brunet et al., 2005), are consistent with the hypothesis that a single species was represented in these collections. Currently described remains assigned to *S. tchadensis* sample from six to nine adult individuals from three fossiliferous localities (TM 247, 266 and 292) scattered across ca. 0.73 km^2 (Brunet et al., 2002, 2005). Cosmogenic nuclide ($^{10}Be/^{9}Be$) dating methods suggest that the Toros-

Menalla localities are older than 6.83 ± 0.45 Ma and younger than 7.04 ± 0.18 Ma (Lebatard et al., 2008), which would place them at the older end of the biochronology-derived ca. 7–6 Ma range (Vignaud et al., 2002). The cosmogenic nuclide ages assume the fossils were found in situ in the sediments. Brunet et al. (2004) implied that part of the holotype cranium was still partly buried when it was discovered, but this has been disputed by Beauvilain and Watté (2009).

The cranium of *S. tchadensis*, while relatively complete, is distorted, and many areas are permeated by matrix-filled cracks. Nonetheless, what is preserved displays a novel combination of primitive (i.e., African ape-like) and derived (i.e., later hominin-like) features (Guy et al., 2005). Much about the cranial base and neurocranium, including its estimated endocranial volume (360–370 cm^3; Zollikofer et al., 2005), is African ape-like, as is the subocclusal mandibular dental morphology (Emonet et al., 2014). Notable exceptions in the cranium are the supraorbital torus, the more horizontal nuchal plane, and the location of the foramen magnum. Although in its recovered state the foramen magnum of the TM 266 cranium is more anteriorly placed than is generally the case in chimpanzees, it is located in the zone of overlap between the ranges for bonobos and modern humans (Ahern, 2005). The presence of a supraorbital torus integrated into the cranial vault, combined with a relatively flat lateral profile of the face, small, apically-worn canines, molar teeth with low, rounded cusps and relatively thick enamel, and a relatively thick mandibular corpus, were all cited by its discoverers as features that excluded *S. tchadensis* from any close relationship with the *Pan* clade (Brunet et al., 2002; Guy et al., 2005).

Zollikofer et al. (2005) attempted to overcome the problems posed by the distortion and matrix-filled cracking by applying the techniques of virtual reconstruction—images based on CT scans manipulated using sophisticated computer software—to the TM 266 cranium. They claimed that the virtually-reconstructed cranium strengthened the case for *S. tchadensis* being an early hominin

by showing that it requires substantial adjustments in multidimensional size–shape space to transform TM 226 into either a *Pan*-like, or a *Gorilla*-like, cranium (Zollikofer et al., 2005: Fig. 3). They also used "minimum form change" (Zollikofer et al., 2005: 755) as evidence to refute the hypothesis that *S. tchadensis* is a fossil gorillin (Wolpoff et al., 2002, 2006). However, if we accept their use of relative "minimum form change" as a taxonomic discriminator, then it would self-evidently involve even more substantial adjustments in multidimensional size–shape space to convert the TM 266 cranium into a modern human cranium, so if we use the same logic Zollikofer et al. (2005) used to argue the TM 266 cranium was not that of a fossil gorillin, then it is even less likely to be a hominin. When Guy et al. (2005) used 3DGM landmark-based methods to capture and compare the morphology of the TM 266 cranium with extant and fossil taxa, their assessment of the implications of the virtually-reconstructed cranium was more nuanced. While they stated that "*Sahelanthropus tchadensis* is clearly a hominid" (a hominin in our usage; Guy et al., 2005: 18840), they also acknowledged that some aspects of its cranial morphology such as the "anteroinferiorly sloping midfacial contour in the midsagittal plane" and "shortened rostrum with substantial projection of the upper face relative to the neurocranium" (Guy et al., 2005: 18838), are either novel morphological features, or novel combinations of features, and they also cautioned that some similarities with fossil hominins, such as the features the TM 266 cranium shares with KNM-ER 1813, could be "either primitive or convergent with *Homo*" (Guy et al., 2005: 18839). In the virtually rendered TM 266 cranium it is noteworthy that the reconstructed angle between the foramen magnum and the orbital plane is closer to the values typical of *Homo sapiens* than to those of australopiths (Zollikofer et al., 2005: Fig. 4). In a recent phylogenetic analysis using an updated version of the craniodental character matrix used by Strait and Grine (2004), Mongle et

al. (2019) concluded that the bootstrap support for *S. tchadensis* being a hominin was absolutely low (41%), and relatively low compared to the bootstrap support for *Ardipithecus ramidus* (64%).

So, given the difficulties of inferring the characteristic morphology of a taxon with a relatively meager fossil record (Smith, 2005), and the fact that the nature and relationships of *S. tchadensis* rely on morphological evidence from a distorted cranium, or from a virtually-reconstructed version of that cranium, any additional information, especially from anatomical regions not sampled in the existing hypodigm, has the potential to help clarify the evolutionary relationships of *S. tchadensis.* Specifically, the current hypodigm of *S. tchadensis* does not include any postcranial remains that might be informative about the posture and locomotion of *S. tchadensis* (Brunet et al., 2002, 2004, 2005; Brunet and Jaeger, 2017). The purpose of this contribution is to introduce the first postcranial evidence of *S. tchadensis.*

1.1. The partial femur TM 266-01-063

According to Beauvilain and Watté (2009), a partial left femur (TM 266-01-063, hereafter the TM 266 femur) was collected on 19th July 2001 at locality TM 266 (16°15'12"' N; 17°29'29" E) in the same location as the holotype TM 266 cranium. It was recognized as a probable primate femur in 2004 when one of us (A.B-M.) was reviewing the collection of nonhominin vertebrate fossils temporarily stored at the University of Poitiers as part of a taphonomic survey of the late Miocene assemblages from Toros-Menalla (Bergeret, 2004). We do not know the present whereabouts of the TM 266 femur.

The ca. 250 mm-long specimen (Fig. 1) consists of a relatively well-preserved and robust left femoral shaft. It lacks any gross morphological evidence that could confirm its maturity. In

addition to longitudinal cracks on the shaft, and some erosion at the distal end, there is evidence of surface weathering and damage consistent with gnawing by a carnivore. As with other fossils from this locality at Toros-Menalla, the TM 266 femur was partially covered by a crust of iron and manganese oxides, beneath which the bone surface is roughened. The original shaft morphology is well-preserved proximally, but the distal end is damaged and slightly compressed anteroposteriorly. The proximal fracture surface preserves the base of the femoral neck, including the distal part of the lesser trochanter (Fig. 2). Enough is preserved to indicate a range of possible neck-shaft angles (Supplementary Online Material [SOM] Fig. S1), but we emphasize that any firm statements about the angulation of the neck are not possible. We estimate the distal break is close to what would have been the junction between the diaphysis and the distal epiphysis: a reasonable estimate of the biomechanical length (Ruff, 2002) of the TM 266 femur is >280 mm (SOM Fig. S2).

Given that the fossil assemblage from Toros-Menalla includes both hyaenids (e.g., *Chasmaporthetes*, *Belbus*, *Hyaenictitherium* and *Werdelinus*) and felids (e.g., *Dinofelis*, *Machairodus*, *Lokotunjailurus* and *Tchadailurus*; Vignaud et al., 2002; Bonis et al., 2005, 2007, 2010a, b; Peigné et al., 2005; Le Fur et al., 2014), we explored the possibility that the TM 266 femur belongs to a carnivoran. However, in carnivorans the neck-shaft angle is usually lower, the proximal shaft is typically not anteroposteriorly flattened, and the intertrochanteric region has a characteristically medially-directed crest that should have been apparent in what is preserved of the lesser trochanter. The TM 266 femoral shaft is convex anteroposteriorly throughout its length. Carnivoran femora are also bowed, but normally only in the distal part of the shaft (Pale and Lambert, 1971; Werdelin and Lewis, 2001; Werdelin, 2003; France, 2011; see also https://www.archeozoo.org/archeozootheque/). For these reasons, we consider it much more likely

that the TM 266 femoral shaft belongs to a primate than to a carnivoran. Given that the only other fossil evidence for a large-bodied primate has been assigned to *S. tchadensis,* and that the TM 266 cranium and the femur were found in the same location (Beauvilain and Watté, 2009: Fig. 1a), it is a reasonable working assumption that the TM 266 femur should also be assigned to *S. tchadensis*.

2. Materials and methods

2.1. Comparative materials

The comparative data used in the analyses include measurements taken from the partial femora BAR 1002'00 and BAR 1003'00, representing *O. tugenensis*, and from samples representing australopiths (*Australopithecus* and *Paranthropus*), modern humans (*H. sapiens*) and extant great apes (*Pan*, *Gorilla*, *Pongo*). Two late Miocene great apes, *Rudapithecus hungaricus* and *Hispanopithecus laietanus*, were also included in the comparative analysis of the cross-sectional shape of the distal femoral shaft (see below).

Measurements of the two *O. tugenensis* femora in Table 1, and the data used in the analysis of the shaft curvature, are based on CT-images whose technical characteristics are detailed in Galik et al. (2004). Additional measurements of BAR 1002'00 and BAR 1003'00 were taken from Senut et al. (2001), Pickford et al. (2002), Nakatsukasa et al. (2007), Puymerail (2011, 2017, and original data).

The australopith sample used in Table 1, which includes representatives of *Au. afarensis*, *Au. africanus*, *Au. sediba*, *P. robustus* and presumed *P. boisei*, consists of the following specimens:

A.L. 128-1, A.L. 152-2, A.L. 333-131, A.L. 333-142, A.L. 827-1 (Ward et al., 2012); A.L. 129-1 (Johanson and Coppens, 1976); A.L. 211-1 (Harmon, 2006); A.L. 288-1ap (Johanson et al., 1982; Haeusler and McHenry, 2004); MAK-VP 1/1 (Lovejoy et al., 2002); StW 573 (Heaton et al., 2019); SK 82, SK 97, StW 99, and U.W. 88-4,5,39 (MH1) (measured by D.M. on the originals; Marchi et al., 2017); A.L. 333-3 and KNM-ER 738 (measured by D.M. on a high-quality cast at the Evolutionary Studies Institute, University of the Witwatersrand, Johannesburg, South Africa; Marchi et al., 2017). Data from the X-ray microtomographic (μXCT) record of the left femur of the A.L. 288-1ap *Au. afarensis* partial skeleton (Johanson et al., 1982; Ruff et al., 2016) was also included in the comparative analysis of the distal cross-sectional shape (courtesy of C.B. Ruff and J.W. Kappelman).

Data for modern humans come from several sources. Ninety-six adult individuals of both sexes from the Bronze Age necropolis of Olmo di Nogara, northern Italy, stored at the Department of Biology, University of Pisa, were used in Table 1 (D.M., personal data). Data from μXCT images (generated at the South African Nuclear Energy Corporation SOC Ltd, Pelindaba, South Africa) of 10 adult individuals (5 females/5 males) of African (n=4) and European (n=6) ancestry from the Pretoria Bone Collection, Pretoria, South Africa, were used in the comparative analysis of the shaft curvature, and in the analysis of distal cross-sectional shape.

Common chimpanzee data include measurements from 42 adult individuals (22 females/20 males) from: the Cleveland Museum of Natural History, Cleveland, USA; the Harvard Museum of Comparative Zoology, Harvard, USA; the Smithsonian Institution's National Museum of Natural History, Washington, D.C., USA; and the Yale Peabody Museum of Natural History, New Haven, USA, used in Table 1 (Marchi et al., 2017). Data from 22 adult individuals (12 females/8 males/2 unknown) from the Digital Morphology Museum, Kyoto University Primate Research

Institute (KUPRI), Japan, 17 individuals from the Izu Shaboten Zoo and the Kyoto City Zoo; http://dmm.pri.kyoto-u.ac.jp/dmm/WebGallery/index.html), one individual from the Evolutionary Studies Institute, University of the Witwatersrand, Johannesburg, South Africa, scanned at the South African Nuclear Energy Corporation SOC Ltd, Pelindaba, South Africa), and four individuals from the Smithsonian Institution's National Museum of Natural History, Washington, D.C., USA (MorphoSource, https://www.morphosource.org/), were used in Table 1 and in the analyses of the shaft curvature and distal cross-sectional shape.

Gorillas data from 47 adult individuals (20 females/27 males) from the Cleveland Museum of Natural History, Cleveland, USA; the Harvard Museum of Comparative Zoology, Harvard, USA; the Smithsonian Institution's National Museum of Natural History, Washington, D.C., USA; and the Yale Peabody Museum of Natural History, New Haven, USA were used in Table 1 (Marchi et al., 2017). Data from the surface model/CT record of 20 adult individuals (9 females/11 males) from the Digital Morphology Museum, Kyoto University Primate Research Institute (KUPRI), Japan, four individuals from the Higashiyama Zoo, the Fukuoka City Zoo and the Kobe Oji Zoo; http://dmm.pri.kyoto-u.ac.jp/dmm/WebGallery/index.html), ten individuals from the Powell-Cotton Museum, Birchington-on-Sea, UK scanned at the Cambridge Biotomography Centre, Department of Zoology, University of Cambridge, Cambridge, UK, and six individuals from the Smithsonian Institution's National Museum of Natural History, Washington, D.C., USA; MorphoSource, https://www.morphosource.org/) were used in Table 1 and in the analyses of the shaft curvature and distal cross-sectional shape.

Orangutan surface model/CT data from five adult (2 females/3 males) and 3 juvenile (1 female/2 males) individuals from the Digital Morphology Museum, Kyoto University Primate Research Institute (KUPRI), Japan (http://dmm.pri.kyoto-u.ac.jp/dmm/WebGallery/index.html),

and seven individuals from the Smithsonian Institution's National Museum of Natural History, Washington, D.C., USA (MorphoSource, https://www.morphosource.org/) were used in Table 1 (adults only). Data used for the analysis of shaft curvature and distal cross-sectional shape come from 10 femora belonging to six individuals (i.e., eight femora are from both sides of four individuals).

In the comparative analysis of the cross-sectional shape of the distal femoral shaft, we also integrated the µXCT-based evidence from *Rudapithecus hungaricus*, from Hungary (Kordos and Begun, 2001; Begun et al., 2012; Ward et al., 2019), and *Hispanopithecus laietanus*, from Spain (Moyà-Solà and Köhler, 1996; Köhler et al., 2002; Almécija et al., 2013; Pina, 2016). *Rudapithecus* is represented by the right femur RUD 184 (courtesy of D.R. Begun and R. Martin), while *Hispanopithecus* by the left femur IPS18800.28 (courtesy of M. Pina and of the Institut Català de Paleontologia Miquel Crusafont).

2.2. Methods

The neck-shaft angle (i.e., between the long axis of the preserved shaft and the axis through the midpoint of the preserved base of the neck; cf. Köhler et al., 2002) was measured using ImageJ (Schneider et al., 2012) on different images of TM 266 in posterior view. Comparative values of the neck-shaft angle for *Pan*, *Gorilla* and *Pongo* in Table 1 are a combination of our original (µ)XCT-based measurements and data from Pina (2016).

For the assessment of the biomechanical length of the TM 266 femur, the 80% cross-sectional level was defined as ca. 1 cm below the distal edge of the lesser trochanter, and the section at 50% (midshaft) at the point of maximum anteroposterior flexion of the shaft in medial and lateral views

(Ruff et al., 1999; Ruff, 2000, 2002; Puymerail et al., 2012). Accordingly, the 20% cross section has been established at approximately 2 cm from the distal-most point of the preserved shaft (SOM Fig. S2).

For assessing the degree of anteroposterior curvature of the femoral shaft, we performed bi-dimensional geometric morphometric (2D GM) analyses on the sketch of TM 266 (SOM Fig. 3) and on the similarly-oriented virtual rendering of BAR 1002'00 (*Orrorin*), and on four (µ)XCT-based records representing *H. sapiens*, *Pan*, *Gorilla* and *Pongo*. The images were imported in TpsUtil64 (Rohlf, 2005) to create a .tps file. Using the TpsDig2 software (Rohlf, 2005), a total of 25 equidistant semilandmarks were digitized along the anterior outline between the point projected from the middle of the lesser trochanter (*a*, estimated in TM 266) and ca. 40% of the biomechanical length (*b*, estimated in both TM 266 and BAR 1002'00 and measured in all other specimens). We then performed generalized Procrustes analyses and a principal component analysis (PCA) and computed the between-group PCA analyses (bgPCA) based on the Procrustes residuals and using the extant taxa as groups. TM 266 and BAR 1002'00 were projected a posteriori in the bgPCA. The analyses were performed using the package ade4 v.1.7-6 (Dray and Dufour, 2007) for R v.3.6.3 (R Development Core Team, 2020).

To assess the cross-sectional morphology of the TM 266 shaft at its naturally-broken distal end (Fig. 2a), which is ca. 15% of the biomechanical length, we firstly extracted the cortical shell by manual delimitation of the endosteal and periosteal contours (SOM Fig. 4a). However, given some damage and the slight anteroposterior compression in the distal shaft, in order to perform a 2D GM-based analysis of the cross-sectional morphology similar to that of the degree of anteroposterior curvature, we generated and projected a posteriori in the analysis two outlines of the TM 266 shaft approximating its original contour in two ways (SOM Fig. 4b, c). For

comparison, we virtually extracted the contours at 15% and 20% of the biomechanical length of the same (μ)XCT-based records of femora representing *H. sapiens*, *Pan*, *Gorilla* and *Pongo*. In this bgPCA analysis we also introduced the section at ca. 20% of the biomechanical length of A.L. 288-1ap (*Au. afarensis*; SOM Fig. 5a), those at ca. 17% and ca. 20% of IPS18800.28 (*Hispanopithecus*; SOM Fig. 5b, c), and that at ca. 20% of RUD 184 (*Rudapithecus*; SOM Fig. 5d). The contours of IPS18800.28 did not require any correction, but the contour of RUD 184 was partially reconstructed to compensate for lateral damage and anteroposterior deformation (SOM Fig. 5d). A total of 80 equidistant semilandmarks were digitized around the outer outline of each cross section used in the analysis.

3. Results

3.1. Comparative analysis

The size and morphology of the TM 266 femoral shaft are much more consistent with it belonging to a fossil hominid than to a fossil monkey, but does it resemble any extant ape? In terms of size and shape, the external morphology of the shaft is closer to that of the common chimpanzee than to modern humans, gorillas or orangutans (Table 1). This is most evidently the case when we consider the anteroposterior curvature and the cross-sectional morphology of the shaft. The results of the bgPCA for the anteroposterior curvature (Fig. 3) locate TM 266 in the same shape space as *Pan*. The analysis also tends to separate *Pongo*, mostly in the positive values of bgPC1, from the other extant hominids, mostly in the negative values (or in the negative values close to the axis origin). *Pongo* is distinguished by an outline which is slightly concave proximally and nearly flat

distally, whereas the other extant hominids show an outline that is flat proximally and more convex distally. Along bgPC2, *Homo* and *Pongo* (mostly in the positive values) are partially discriminated from *Gorilla* and *Pan* (mostly in the negative values) by a slightly convex, or even nearly flat shape, distinct from the more sinusoidal outline of the African apes. TM 266 and BAR 1002'00 (*Orrorin*) are at different locations in this morphospace: TM 266 is within the variation of *Pan*, near that of *Gorilla*, and outside the morphospace occupied by *Homo* and *Pongo*, while BAR 1002'00 falls between *Homo* and *Pongo*, and away from the African ape morphospace (Fig. 3).

Likewise, the cross-sectional morphology of the TM 266 distal shaft (Fig. 2a) is most similar to that of *Pan* (Fig. 4). Indeed, in the morphospace of the bgPCA (Fig. 5), the sub-ovoidal cross-sectional outlines of TM 266 and *Rudapithecus* are distinct from all of the extant hominids, except *Pan*, while the more anteroposteriorly compressed outline of *Hispanopithecus* is separate from modern humans, far from that of *Pan*, and closer to the morphology of *Pongo* and *Gorilla*. In this context, it is noteworthy that the closest fit for the sub-rounded cross section of *Au. afarensis* are extant humans (Fig. 5).

The neck-shaft angle estimated from the preserved morphology (Fig. 2b) ranges between 138° and 146° (SOM Fig. S1). If we use the conservative estimate of >135° provided in Table 1, the angle in TM 266 is likely to have been higher than in BAR 1002'00, and above the range seen in the extant African apes (Table 1). It was likely closer to the range of values for *Pongo* and *Hispanopithecus* (Köhler et al., 2002; Pina, 2016).

The TM 266 femoral shaft is larger at all comparable cross-sectional levels than the average for *Pan* (Table 1), but the reconstructed biomechanical length is similar to the estimates for *O. tugenensis* (BAR 1002'00: 288 mm; BAR 1003'00: 297 mm; Nakatsukasa et al., 2007; Puymerail, 2017 and original data). This suggests that the body mass of the TM 266 individual likely exceeded

the ca. 47 kg estimated for the body mass of BAR 1003'00, the larger of the two better-preserved *O. tugenensis* femora (Grabowski et al., 2018; see also Nakatsukasa et al., 2007).

3.2. Functional assessment

An erect posture and bipedal locomotion have traditionally been accepted as one of the defining features of the hominin clade (e.g., Le Gros Clark, 1955), and they are routinely used as criteria to assess whether Pliocene hominid fossils should be included in the hominin clade (e.g., Haile-Selassie et al., 2004; White et al., 2009; Simpson, 2013; Pilbeam and Lieberman, 2017). That is not to say that all habitually bipedal hominids are necessarily hominins, but the consensus is that to be a member of the hominin clade the morphology of a candidate species needs to be consistent with habitual bipedalism. If it could be demonstrated that the morphology of the TM 266 femoral shaft was consistent with its owner being an habitual biped, this would strengthen the case for it being a hominin.

There are at least two lines of evidence that can be pursued to investigate this. First, is the morphology of TM 266 more similar to the only extant habitual biped, modern humans, than to closely-related extant taxa that do not practise habitual bipedalism? Given the results of the comparative analyses in the previous section, the overall morphology of TM 266 appears to be closer to that of common chimpanzees than it is to habitually bipedal modern humans. In addition, in bipedal hominins with medial angulation of the shaft associated with a valgus knee, there is a reduction in shaft width as you move from the subtrochanteric to the midshaft level (i.e., distally within the 80–50% portion of the estimated femoral biomechanical length; Ruff et al., 2016). The TM 266 femoral shaft lacks this distal taper.

But we know the hominin clade includes taxa that are almost certainly habitual bipeds, yet their femoral morphology differs from that of modern humans (Lovejoy and Heiple, 1972; Richmond and Jungers, 2008). Unfortunately, the TM 266 femur lacks the regions—the proximal and distal epiphyses—that are most informative about the functional role (sensu Bock and von Wahlert, 1965) of the femur (e.g., Lovejoy, 1988; Richmond and Jungers, 2008; Ruff and Higgins, 2013; Marchi et al., 2017; Cazenave et al., 2019; Pina et al., 2019; Sukhdeo et al., 2020). Although the proximal epiphysis is missing in TM 266, the proximal end of BAR 1002′00, the most complete of the three partial femora attributed to *O. tugenensis* (Senut et al., 2001; Pickford et al., 2002), is relatively complete and well preserved (Fig. 6). Its external and internal morphology have been the subject of relatively intensive investigation, with most authors concluding that BAR 1002′00 is consistent with australopith-like habitual bipedalism (Pickford et al., 2002; Galik et al., 2004; Nakatsukasa et al., 2007; Richmond and Jungers, 2008, 2012; Kuperavage et al., 2018). Exceptions to this consensus are Almécija et al. (2013), who saw differences between the bipedalism of BAR 1002′00 and australopiths, and Ohman et al. (2005), who questioned the interpretation of the internal morphology. Bleuze (2012) conducted a comparative study using the cross-sectional geometry of the proximal end of the femoral shaft, and concluded that BAR 1002′00 and BAR 1003′00 resemble the australopiths. So, if the BAR 1002′00 femur belongs to an habitual biped, and if the parts of the femur that are preserved in common in TM 266 and BAR 1002′00 resemble each other as closely as two members of the same taxon, then this would be a second line of evidence in support of the hypothesis that *S. tchadensis* is a habitual biped. The results of our preliminary analysis of anteroposterior curvature suggest the opposite, in that the difference in anteroposterior curvature in multivariate space between TM 266 and BAR 1002′00 exceeds the variation we see within any of the extant great apes (Fig. 3).

The functional implications of the non-metrical morphology of the TM 266 femur are less clear. There is no spiral line, nor is there a gluteal tuberosity. Intertrochanteric and spiral lines are both evident in BAR 1002'00, and both BAR 1002′00 and BAR 1003′00 have a gluteal tuberosity (Pickford et al., 2002). However, the evolutionary significance of the latter is unclear, for while it is usually absent in extant African apes (Lovejoy et al., 2002), it is present in some Miocene apes (Nakatsusaka and Kunimatsu, 2004; Almécija et al., 2013; Pilbeam and Lieberman, 2017; Pina et al., 2019). The region that would provide evidence of an intertrochanteric line is missing in TM 266. The presence of the pectineal line, which is marked in *O. tugenensis*, could not be confidently assessed in TM 266 because of damage to the surface bone in that area (Fig. 2b), but there is evidence of a modestly-developed lateral spiral pilaster, a feature common in extant apes (Lovejoy et al., 2002), but absent in *O. tugenensis* (Pickford et al., 2002).

Below the greater trochanter, the posterior surface of the TM 266 femur bears a laterally-convex crest that extends distally to the midline where, proximal to the midshaft, it contributes to a modest linea aspera. More distally the surface topography is poorly preserved (Fig. 2c). The morphology of the posterior surface of the femoral shaft is unlike that seen in BAR 1002'00, which has a salient and wide midline crest on the posterior aspect of the shaft (Senut et al., 2001; Pickford et al., 2002).

Given the broader comparative context of the morphology of the TM 266 femur, there is no compelling evidence that it belongs to a habitual biped, something that would strengthen the case for *S. tchadensis* being a hominin. Indeed, the shape differences between TM 266 and BAR 1002'00 suggest that the locomotor modes of *S. tchadensis* and *O. tugenensis* were different.

4. Discussion

Guy et al. (2005: 18839) suggested that "further research is needed to determine the evolutionary relationships between *Sahelanthropus* and known Miocene and Pliocene hominids", and in the final section of their paper they made a plea for "more information" (Guy et al., 2005: 18840). In relation to claims that evidence from the TM 266 cranium was consistent with *S. tchadensis* being a habitual biped, Richmond and Jungers (2008: 1662) suggested that "postcranial fossils are needed to confirm this conclusion". We review below what can be said about the taxonomy and functional morphology of the TM 266 femoral shaft in descending order of confidence. It is unfortunate that the information provided by the TM 266 femur is limited to the shaft. We would have greater confidence in our taxonomic and functional analysis if that were not the case.

We are most confident that the TM 266 femoral shaft belongs to a hominid sensu lato. It could sample a hominid hitherto unrepresented at Toros-Menalla, but a more parsimonious working hypothesis is that it belongs to *S. tchadensis*. The differences between TM 266 and the *O. tugenensis* partial femur BAR 1002'00 are substantial, and are consistent with maintaining at least a species-level distinction between *S. tchadensis* and *O. tugenensis*, but most of what has been published about the femoral morphology of *O. tugenensis* is based on the analysis of just one, BAR 1002'00, of three femoral specimens assigned to that taxon. Finally, if the TM 266 femoral shaft belongs to *S. tchadensis*, we cannot be confident that the latter was a habitual biped.

We must emphasize that our observations on the TM 266 femoral shaft are preliminary. They are limited to what we can glean from the literature, plus limited and brief access to the original fossil. We hope that those with curatorial responsibility for the original specimen will conduct a more detailed and thorough comparative study, including assessments of cross-sectional geometric properties and internal structure.

406 However, on the assumption that the TM 266 femur is a justified addition to the hypodigm of
407 *S. tchadensis*, what are the implications of our preliminary assessment of the new evidence for the
408 evolutionary relationships of *S. tchadensis*? Does the new evidence have any broader implications
409 for our understanding of hominid and hominin evolution in Africa at this time (i.e., ca. 7–6 Ma)?
410 There are an impressive number of differences between the morphology of
411 chimpanzees/bonobos and modern humans, but the differences between the late Miocene ancestors
412 of modern humans and chimpanzees/bonobos are likely to have been much more subtle. Some of
413 the features that distinguish modern humans from chimpanzees/bonobos, such as those linked with
414 bipedalism, can be traced back a long way (Almécija et al., 2013; Böhme et al., 2019). Others,
415 such as the relatively diminutive jaws and chewing teeth of modern humans, were acquired more
416 recently and thus cannot be used to tell the difference between stem hominins and stem panins.
417 Given these caveats, how do we go about telling a stem hominin from a stem panin? The
418 conventional assumption is that a stem panin would have had a projecting face accommodating an
419 elongated jaw bearing relatively small chewing teeth and relatively and absolutely large, sexually-
420 dimorphic, honed canine teeth, and a locomotor system adapted for arboreal quadrupedalism
421 (Pilbeam and Lieberman, 2017). A stem hominin, on the other hand, would have been
422 distinguished by cranial and other skeletal adaptations to a predominantly upright posture and
423 skeletal and other adaptations for a locomotor strategy that includes substantial bouts of terrestrial
424 bipedalism. These features would been combined with a masticatory apparatus that combines
425 relatively large chewing teeth and modest-sized canines. These inferences are working hypotheses
426 that will need to be reviewed and tested as the relevant evidence is uncovered (Guy et al., 2005).
427 It should be clear from the foregoing that the presence of only one, or even a few, of the features
428 that possibly distinguish early hominins from early panins, may not be sufficient to identify a fossil

as a hominin or a panin. This is because there is evidence that primates, like many other groups of mammals, are affected by homoplasy (aka false homology; Diogo and Wood, 2011). Phenotypic homoplasies are morphological features that are shared by two, or more, taxa that are not seen in the most recent common ancestor of those taxa. The possibility of convergent and/or parallel evolution—both of which can result in homoplasy—means that it is not impossible, indeed it may even be probable, that some of what many have come to regard as key morphological adaptations at the base of the hominin lineage may have arisen more than once. If that is the case, then what characterizes hominins (and panins and the other great ape lineages) may not be particular items of morphology, single characters, but particular combinations of characters.

It is possible that *S. tchadensis* is a stem hominin with some reduction of the canine and loss of the honing complex, but without adaptations to bipedalism. But, being a stem hominin or a stem panin, or their most recent common ancestor, may not be the only options for *S. tchadensis*. Given what we have learned about the evolutionary history of the clade that includes the extant great apes, it is likely, and indeed probable, that during the late Miocene and the early Pliocene there was a modest adaptive radiation of African hominids that includes taxa that are neither hominins or panins as defined above (Wood and Harrison, 2011). Any such extinct groups are likely to include taxa with novel morphology, or with novel combinations of morphology we also see in hominins or panins. Given the mix of inferred primitive and inferred derived features in *S. tchadensis*, we suggest it could belong to a group that has no living representative.

5. Conclusion

The lack of clear evidence that the TM 266 femur is from a hominid that was habitually bipedal further weakens the already weak case (Mongle et al., 2019) for *S. tchadensis* being a stem hominin. However, this in no way diminishes the significance of *S. tchadensis* (Brunet et al., 2002). There is a compelling evidence that, for at least the last four million years, the hominin clade shows evidence of taxonomic, and thus lineage, diversity (Haile-Selassie et al., 2016; Wood and Boyle, 2016). If this is the case, the minority of the extinct hominin taxa that have been recognized are likely to be the ancestors of modern humans; most will turn out to be non-ancestral close relatives. Presently, it is difficult to sort ancestors from non-ancestral close relatives. There is no logical reason to think that the same problems and limitations do not also apply to late Miocene hominids. It will not be easy, especially if the fossil evidence is relatively meager, to work out which late Miocene taxa are hominins, which are panins, and which are neither. If we treat the hominin status of *S. tchadensis*, or any other enigmatic taxon, as a given and not a hypothesis, we run the risk of adding further confusion to a picture that is already "complicated and less easy to resolve" (Guy, et al., 2005: 18839).

Acknowledgements

This contribution benefited from data and interpretations made by L. Puymerail on CT scans of BAR 1002'00 and BAR 1003'00 kindly made available by B. Senut and M. Pickford. For access to comparative materials, scanning facilities, and/or data/information sharing, we acknowledge S. Almécija, A. Beauvilain, D.R. Begun, B. Billings, L. Bondioli, J. Braga, M. Cazenave, J. Chupasko, F. de Beer, J.M. DeSilva, M. Domínguez-Rodrigo, Y. Haile-Selassie, K. Jakata, L. Jellema, J.W. Kappelman, L. Kgasi, T.L. Kivell, E. L'Abbé, I. Livne, R. Martin, B. Martínez-

Navarro, M. Nakatsukasa, S. Peigné, M. Pina, S. Potze, L. Rook, C.B. Ruff, L. Salzani, M.M. Skinner, J.-F. Tournepiche, E. Westwig, C. Zanolli, and B. Zipfel. We also acknowledge the Institut Català de Paleontologia Miquel Crusafont, the Digital Morphology Museum (KUPRI, http://dmm.pri.kyoto-u.ac.jp/dmm/WebGallery/index.html) and the MorphoSource (https://www.morphosource.org/) for access to their 3D databases. The input from three reviewers, two Associate Editors and two Editors was greatly appreciated.

References

Ahern, J.C., 2005. Foramen magnum position variation in *Pan troglodytes*, Plio-Pleistocene hominids, and recent *Homo sapiens*: Implications for recognizing the earliest hominids. American Journal of Physical Anthropology 127, 267-276.

Almécija, S., Tallman, M., Alba, D.M., Pina, M., Moyà-Solà, S. Jungers, W.L., 2013. The femur of *Orrorin tugenensis* exhibits morphometric affinities with both Miocene apes and later hominins. Nature Communications 4, 2888.

Beauvilain, A., Watté, J.-P., 2009. Was Toumaï (*Sahelanthropus tchadensis*) buried? Anthropologie 47, 1-6.

Begun, D.R., Nargolwalla, M.C., Kordos, L., 2012. European Miocene hominids and the origin of the African ape and human clade. Evolutionary Anthropology 21, 10-23.

Bergeret, A., 2004. Approche taphonomique d'un assemblage miocène de vertébrés fossiles du désert du Djourab (Tchad): implications paléoécologiques. DEA Thesis, Université de Poitiers.

Bleuze, M., 2012. Proximal femoral diaphyseal cross-sectional geometry in *Orrorin tugenensis.* Journal of Comparative Human Biology, 63, 153-166.

497 Bock, W., von Wahlert, G., 1965. Adaptation and the form-function complex. Evolution 19, 269-
498 299.
499 Böhme, M., Spassov, N., Fuss, J., Tröscher, A., Deane, A.S., Prieto, J., Kirscher, U., Lechner, T.,
500 Begun, D.R., 2019. A new Miocene ape and locomotion in the ancestor of great apes and
501 humans. Nature 575, 489-493.
502 Bonis, L. de, Peigné, S., Guy, F., Likius, A., Mackaye, H.T., Vignaud, P., Brunet, M., 2010a.
503 Hyaenidae (Carnivora) from the late Miocene of Toros-Menalla, Chad. Journal of African Earth
504 Sciences 58, 561-679.
505 Bonis, L. de, Peigné, S., Likius, A., Mackaye, H.T., Vignaud, P., Brunet, M., 2005.
506 *Hyaenictitherium minimum*, a new ictithere (Mammalia, Carnivora, Hyaenidae) from the Late
507 Miocene of Toros-Menalla, Chad. Comptes Rendus Palevol 4, 671-679.
508 Bonis, L. de, Peigné, S., Likius, A., Mackaye, H.T., Vignaud, P., Brunet, M., 2007. First
509 occurrence of the "hunting hyena" *Chasmaporthetes* in the Late Miocene fossil bearing
510 localities of Toros Menalla Chad (Africa). Bulletin de la Société Géologique de France 178,
511 317-326.
512 Bonis, L. de, Peigné, S., Likius, A., Mackaye, H.T., Vignaud, P., Brunet, M., 2010b. New sabre-
513 toothed cats in the late Miocene of Toros Menalla (Chad). Comptes Rendus Palevol 9, 221-227.
514 Bradley, B., 2008. Reconstructing phylogenies and phenotypes: A molecular view of human
515 evolution. Journal of Anatomy 212, 337-353.
516 Brunet, M., Guy, F., Boisserie, J.-R., Djimdoumalbaye, A., Lehmann, T., Lihoreau, F., Louchart,
517 A., Schuster, M., Tafforeau, P., Likius, A., Mackaye, H.T., Blondel, C., Bocherens, H., de
518 Bonis, L., Coppens, Y., Denis, C., Duringer, P. Eisenmann, V., Flisch, A., Geraads, D., Lopez-
519 Martinez, N., Otero, O., Peláez-Campomanes, P., Pilbeam, D., Ponce de León, M.S., Vignaud,

P., Viriot, L., Zollikofer, C., 2004. "Toumaï", Miocène supérieur du Tchad, le nouveau doyen du rameau humain. Comptes Rendus Palevol 3, 277-285.

Brunet, M., Guy, F., Pilbeam, D., Lieberman, D.E., Likius, A., Mackaye, H.T., Ponce de León, M.S., Zollikofer, C., Vignaud, P., 2005. New material of the earliest hominid from the Upper Miocene of Chad. Nature 434,752-755.

Brunet, M., Guy, F., Pilbeam, D., Mackaye, H.T., Likius, A., Ahounta, D., Beauvilain, A., Blondel, C., Bocherens, H., Boisserie, J.-R., de Bonis, L., Coppens, Y., Dejax, J., Denys, C., Duringer, P., Eisenmann, V., Gongdibe, F., Fronty, P., Geraads, D., Lehmann, T., Lihoreau, F., Louchart, A., Mahamat, A., Merceron, G., Mouchelin, G., Otero, O., Peláez -Campomanes, P., Ponce de León, M.S., Rage, J.-C., Sapanet, M., Schuster, M., Sudre, J., Tassy, P., Valentin, X., Vignaud, P., Viriot, L., Zazzo, A., Zollikofer, C., 2002. A new hominid from the Upper Miocene of Chad, Central Africa. Nature 418,145-151.

Brunet, M., Jaeger, J.-J., 2017. De l'origine des anthropoïdes à l'émergence de la famille humaine. Comptes Rendus Palevol 16, 189-195.

Cazenave, M., Braga, J., Oettlé, A., Pickering, T.R., Heaton, J.L., Nakatsukasa, M., Thackeray J.F., de Beer, F., Hoffman, J., Dumoncel, J., Macchiarelli, R., 2019. Cortical bone distribution in the femoral neck of *Paranthropus robustus*. Journal of Human Evolution 135, 102666.

Diogo, R., Molnar, J.L., Wood, B., 2017. Bonobo anatomy reveals stasis and mosaicism in chimpanzee evolution, and supports bonobos as the most appropriate extant model for the common ancestor of chimpanzees and humans. Scientific Reports 7, 608.

Diogo, R., Wood, B., 2011. Soft-tissue anatomy of the primates: phylogenetic analyses based on the muscles of the head, neck, pectoral region and upper limb, with notes on the evolution of these muscles. Journal of Anatomy 219, 273–359.

543 Dray, S., Dufour, A.B., 2007. The ade4 package: Implementing the duality diagram for ecologists.
544 Journal of Statistical Software 22, 1-20.
545 Emonet, E.-G., Andossa, L., Mackaye, H.T., Brunet, M., 2014. Subocclusal dental morphology of
546 *Sahelanthropus tchadensis* and the evolution of teeth in hominins. American Journal of
547 Physical Anthropology 153, 116-123.
548 France, D.L., 2011. Human and Nonhuman Bone Identification. A Concise Field Guide. CRC
549 Press, Boca Raton.
550 Galik, K., Senut, B., Pickford, M., Gommery, D., Treil, J., Kuperavage, A.J., Eckhardt, R.B., 2004.
551 External and internal morphology of the BAR 1002000 *Orrorin tugenensis* femur. Science 305,
552 1450-1453.
553 Grabowski, M., Hatala, K.G., Jungers, W.L., 2018. Body mass estimates of the earliest possible
554 hominins and implications for the last common ancestor. Journal of Human Evolution 122, 84-
555 92.
556 Guy, F., Lieberman, D.E., Pilbeam, D., Ponce de León, M., Likius, A., Mackaye, H.T., Vignaud,
557 P., Zollikofer, C., Brunet, M., 2005. Morphological affinities of the *Sahelanthropus tchadensis*
558 (Late Miocene hominid from Chad) cranium. Proceedings of the National Academy of Sciences
559 USA 102, 18836-18841.
560 Haeusler, M., McHenry, H.M., 2004. Body proportions of *Homo habilis* reviewed. Journal of
561 Human Evolution 46, 433-465.
562 Haile-Selassie, Y., Melillo, S.M., Su, D.F., 2016. The Pliocene hominin diversity conundrum: Do
563 more fossils mean less clarity? Proceedings of the National Academy of Sciences USA 113,
564 6364-6371.

565 Haile-Selassie, Y., Suwa, G., White, T.D., 2004. Late Miocene teeth from Middle Awash,
566 Ethiopia, and early hominid dental evolution. Science 303, 1503-1505.
567 Harmon, E.H., 2006. Size and shape variation in *Australopithecus afarensis* proximal femora.
568 Journal of Human Evolution 51, 217-227.
569 Heaton, J.L., Pickering, T.R., Carlson, K.J., Crompton, R.H., Jashashvili, T., Beaudet, A.,
570 Bruxelles, L., Kuman, K., Heile, A.J., Stratford, D., Clarke, R.J., 2019. The long limb bones of
571 the StW 573 *Australopithecus* skeleton from Sterkfontein Member 2: Descriptions and
572 proportions. Journal of Human Evolution 133, 167-197.
573 Johanson, D.C., Coppens, Y., 1976. A preliminary anatomical diagnosis of the first
574 Plio/Pleistocene hominid discoveries in the Central Afar, Ethiopia. American Journal of
575 Physical Anthropology 45, 217-234.
576 Johanson, D.C., Lovejoy, C.O., Kimbel W.H., White, T.D., Ward, S.C., Bush, M.E., Latimer,
577 B.M., Coppens, Y., 1982. Morphology of the Pliocene partial hominid skeleton (A.L. 288-1)
578 from the Hadar formation, Ethiopia. American Journal of Physical Anthropology 57, 403-451.
579 Köhler, M., Alba, D.M., Moyà, S., MacLatchy, L., 2002. Taxonomic affinities of the Eppelsheim
580 femur. American Journal of Physical Anthropology 119, 297-304.
581 Kordos, L., Begun, D.R., 2001. Primates from Rudabánya: Allocation of specimens to individuals,
582 sex and age categories. Journal of Human Evolution 40, 17-39.
583 Kuperavage, A., Pokrajac, D., Chavanaves, S., Eckhardt, R.B., 2018. Earliest known hominin
584 calcar femorale in *Orrorin tugenensis* provides further internal anatomical evidence for origin
585 of human bipedal locomotion. The Anatomical Record 30, 1834-1839.
586 Langergraber, K.E., Prüfer, K., Rowney, C., Boesch, C., Crockford, C., Fawcett, K., Inoue, E.,
587 Inoue-Muruyama, M., Mitani, J.C., Muller, M.N., Robbins, M.M., Schubert, G., Stoinski, T.S.,

588 Viola, B., Watts, D., Wittig, R.M., Wrangham, R.W., Zuberbühler, Pääbo, S., Vigilant, L.,
589 2012. Generation times in wild chimpanzees and gorillas suggest earlier divergence times in
590 great ape and human evolution. Proceedings of the National Academy of Sciences USA 109,
591 15716-15721.
592 Lebatard A.-E., Bourlès, D.L., Duringer, P., Jolivet, M., Braucher, R., Carcaillet, J., Schuster, M.,
593 Arnaud, N., Monié, P., Lihoreau, F., Likius, A., Mackaye, H.T., Vignaud, P., Brunet, M., 2008.
594 Cosmogenic nuclide dating of *Sahelanthropus tchadensis* and *Australopithecus bahrelghazali*:
595 Mio-Pliocene hominids from Chad. Proceedings of the National Academy of Sciences USA
596 105, 3226-3231.
597 Le Fur, S., Fara, E., Mackaye, H.T., Vignaud, P., Brunet, M., 2014. Toros-Menalla (Chad, 7 Ma),
598 the earliest hominin-bearing area: How many mammal paleocommunities? Journal of Human
599 Evolution 69, 79-90.
600 Le Gros Clark, W.E., 1955. The Fossil Evidence for Human Evolution: An Introduction to the
601 Study of Paleoanthropology. University of Chicago Press, Chicago, IL.
602 Lovejoy, C.O., 1988. Evolution of Human Walking. Scientific American 259(5), 118-125.
603 Lovejoy, C.O., Heiple, K.G., 1972. Proximal femoral anatomy of *Australopithecus*. Nature 235,
604 175-176.
605 Lovejoy, C.O., Meindl, R.S., Ohman, J.C., Heiple, K.G., White, T.D., 2002. The Maka femur and
606 its bearing on the antiquity of human walking: Applying contemporary concepts of
607 morphogenesis to the human fossil record. American Journal of Physical Anthropology 119,
608 97-133.
609 Marchi, D., Walker, C.S., Wei, P., Holliday, T.W., Churchill, S.E., Berger, L.R., DeSilva, J.M.,
610 2017. The thigh and leg of *Homo naledi*. Journal of Human Evolution 104, 174-204.

611 Mongle, C.S., Strait, D.S., Grine, F.E., 2019. Expanded character sampling underscores
612 phylogenetic stability of *Ardipithecus ramidus* as a basal hominin. Journal of Human Evolution
613 131, 28-39.
614 Moorjani, P., Sankararaman, S., Fu, Q., Przeworski, M., Patterson, N., Reich, D., 2016. A genetic
615 method for dating ancient genomes provides a direct estimate of human generation interval in
616 the last 45,000 years. Proceedings of the National Academy of Sciences USA 113, 5652-5657.
617 Moyà-Solà, S., Köhler, M., 1996. A *Dryopithecus* skeleton and the origin of great-ape locomotion.
618 Nature 379, 156-159.
619 Nakatsusaka, M., Kunimatsu, Y., 2004. *Nacholapithecus* and its importance for understanding
620 hominoid evolution. Evolutionary Anthropology 18, 103-119.
621 Nakatsukasa, M., Pickford, M., Egi, N., Senut, B., 2007. Femur length, body mass, and stature
622 estimates of *Orrorin tugenensis*, a 6 Ma hominid from Kenya. Primates 48, 171-178.
623 Ohman, J.C., Lovejoy, C.O., White, T.D., 2005. Questions about *Orrorin* femur. Science 307, 845.
624 Pale, L., Lambert, C., 1971. Atlas Ostéologique pour Server à l'Identification des Mammifères du
625 Quaternarire. I. Les Membres. Carnivores. Editions CNRS, Paris.
626 Peigné, S., Bonis, L. de, Likius, A., Mackaye, H.T., Vignaud, P., Brunet, M., 2005. New
627 machairodontine (Carnivora, Felidae) from the Late Miocene hominid of Toros-Menalla Chad.
628 Comptes Rendus Palevol 4, 243-253.
629 Pickford, M., Senut, B., Gommery, D., Treil, J., 2002. Bipedalism in *Orrorin tugenensis* revealed
630 by its femora. Comptes Rendus Palevol 1, 1-13.
631 Pilbeam, D.R., Lieberman, D.E., 2017. Reconstructing the last common ancestor of chimpanzees
632 and humans. In: Muller, M.N., Wrangham, R.W., Pilbeam, D.R. (Eds), Chimpanzees and
633 Human Evolution. Belknap Press of Harvard University Press, Cambridge, MA., pp. 22-141.

Pina, M., 2016. Unraveling the positional behaviour of fossil hominoids: Morphofunctional and structural analysis of the primate hindlimb. Ph.D. Dissertation, Universitat Autònoma de Barcelona.

Pina, M., Alba, D.M., Moyà-Solà, S., Almécija, S., 2019. Femoral neck cortical bone distribution of dryopithecin apes and the evolution of hominid locomotion. Journal of Human Evolution 136, 102651.

Prado-Martinez, J., Sudmant, P.H., Kidd, J.M., Li, H., Kelley, J.L., Lorente-Galdos, B., Veeramah, K.R., Woerner, A.E., O'Connor, T.D., Santpere, G., Cagan, A., Theunert, C., Casals, F., Laayouni, H., Munch, K., Hobolth, A., Halager, A.E., Malig, M., Hernandez-Rodriguez, J., Hernando-Herraez, I., Prüfer, K., Pybus M., Johnstone, L., Lachmann M., Alkan, C., Twigg, D., Petit, N., Baker, C., Hormozdiari, F., Fernandez-Callejo, M., Dabad, M., Wilson, M.L., Stevison, L., Camprubí, C., Carvalho, T., Ruiz-Herrera, A., Vives, L., Mele, M., Abello, T., Kondova, I., Bontrop, R.E., Pusey, A., Lankester, F., Kiyang, J.A., Bergl, R.A., Lonsdorf, E., Myers, S., Ventura, M., Gagneux, P., Comas, D., Siegismund, H., Blanc, J., Agueda-Calpena, L., Gut, M., Fulton, L., Tishkoff, S.A., Mullikin, J.C., Wilson, R.K., Gut, I.G., Gonder, M.K., Ryder, O.A., Hahn, B.H., Navarro, A., Akey, J.M., Bertranpetit, J., Reich, D., Mailund, T., Schierup, M.H., Hvilsom, C., Andrés, A.M., Wall, J.D., Bustamante, C.D., Hammer, M.F., Eichler, E.E., Marques-Bonet, T., 2013. Great ape genetic diversity and population history. Nature 499, 471-475.

Puymerail, L., 2011. Caractérisation de l'endostructure et des propriétés biomécaniques de la diaphyse fémorale: la signature de la bipédie et la reconstruction des paléo-répertoires posturaux et locomoteurs des Hominines. Ph.D. Dissertation, Muséum national d'Histoire naturelle, Paris.

Puymerail, L., 2017. The structural and mechanical properties of the *Orrorin tugenensis* femoral shaft and the assessment of bipedalism in early hominins. In: Macchiarelli, R., Zanolli, C. (Eds), Hominin Biomechanics, Virtual Anatomy and Inner Structural Morphology: From Head to Toe. A Tribute to Laurent Puymerail. Comptes Rendus Palevol 16, 493-498.

Puymerail, L., Ruff, C.B., Bondioli, L., Widianto, H., Trinkaus, E., Macchiarelli, R., 2012. Structural analysis of the Kresna 11 *Homo erectus* femoral shaft (Sangiran, Java). Journal of Human Evolution 63, 741-749.

R Development Core Team, 2020 R: A language and environment for statistical computing. http://www.R-project.org.

Richmond, B.G., Jungers, W.L., 2008. *Orrorin tugenensis* femoral morphology and the evolution of hominin bipedalism. Science 319, 1662-1665.

Richmond, B.G., Jungers, W.L., 2012. Hominin proximal femur morphology from the Tugen Hills to Flores. In: Reynolds, S.C., Gallagher, A. (Eds), African Genesis: Perspectives on Hominin Evolution. Cambridge University Press, Cambridge, pp. 248-267.

Rohlf, F.J., 2005. TpsDig2. TpsSeries. Department of Ecology and Evolution, SUNY, Stony Brook, New York.

Ruff, C.B., 2000. Body size, body shape, and long bone strength in modern humans. Journal of Human Evolution 38, 269-290.

Ruff, C.B., 2002. Long bone articular and diaphyseal structure in Old World monkeys and apes. I: Locomotor effects. American Journal of Physical Anthropology 119, 305-342.

Ruff, C.B., Burgess, M.L., Ketcham, R.A., Kappelman, J., 2016. Limb bone structural proportions and locomotor behavior in A.L. 288-1 ("Lucy"). PLoS One 11, e0166095.

679 Ruff, C.B., Higgins, R., 2013. Femoral neck structure and function in early hominins. American
680 Journal of Physical Anthropology 150, 512-525.
681 Ruff, C.B., McHenry, H.M., Thackeray, J.F., 1999. Cross-sectional morphology of the SK 82 and
682 97 proximal femora. American Journal of Physical Anthropology 109, 509-521.
683 Ruvolo, M., 1997. Molecular phylogeny of the hominoids: Inferences from multiple independent
684 DNA sequence data sets. Molecular Biology and Evolution 14, 248-65.
685 Schneider, C.A., Rasband, W.S., Eliceiri, K.W., 2012. NIH Image to ImageJ: 25 years of image
686 analysis. Nature Methods 9, 671-675.
687 Senut, B., Pickford, M., Gommery, D., Mein, P., Cheboi, K., Coppens, Y., 2001. First hominid
688 from the Miocene (Lukeino Formation, Kenya). Comptes Rendus de l'Académie des Sciences
689 de Paris 332, 137-144.
690 Simpson, S.W., 2013. Before *Australopithecus*: The earliest hominins. In: Begun, D.R. (Ed.), A
691 Companion to Paleoanthropology. Wiley-Blackwell, Malden, pp. 417-433.
692 Smith, R.J., 2005. Species recognition in paleoanthropology; implications of small sample sizes.
693 In: Lieberman, D.E., Smith, R.J., Kelley, J. (Eds), Interpreting the Past: Essays on Human,
694 Primate, and Mammal Evolution in Honor of David Pilbeam. Brill Academic Publishers,
695 Boston, pp. 207-219.
696 Stone, A.C., Battistuzzi, F.U., Kubatko, L.S., Perry Jnr, G.H., Trudeau, E., Lin, H., Kumar, S.,
697 2010. More reliable estimates of divergence times in *Pan* using complete mt DNA sequences
698 and accounting for population structure. Philosophical Transactions of the Royal Society B 365,
699 3277-3288.
700 Strait, D.S., Grine, F.E., 2004. Inferring hominoid and early hominid phylogeny using craniodental
701 characters: the role of fossil taxa. Journal of Human Evolution 47, 399-452.

Sukhdeo, S., Parsons, J., Niu, X.M., Ryan, T.M., 2020. Trabecular bone structure in the distal femur of humans, apes, and baboons. The Anatomical Record 303, 129-149.

Vignaud, P., Duringer, P., Mackaye, H.T., Likius, A., Blondel, C., Boisserie, J.-R., de Bonis, L., Eisenmann, V., Etienne, M.-E., Geraads, D., Guy, F., Lehmann, T., Lihoreau, F., Lopez-Martinez, N., Mourer-Chauviré, C., Otero, O., Rage, J.-C., Schuster, M., Viriot, L., Zazzo, A., Brunet, M., 2002. Geology and paleontology of the Upper Miocene Toros-Menalla hominid locality, Chad. Nature 418, 152-155.

Ward, C.V., Hammond, A.S., Plavcan, J.M., Begun, D.R., 2019. A late Miocene hominid partial pelvis from Hungary. Journal of Human Evolution 136, 102645.

Ward, C.V., Kimbel, W.H., Harmon, E.H., Johanson, D.C., 2012. New postcranial fossils of *Australopithecus afarensis* from Hadar, Ethiopia (1990-2007). Journal of Human Evolution 63, 1-51.

Werdelin, L., 2003. Mio-Pliocene Carnivora from Lothagam, Kenya. In: Leakey, M.G., Harris, J.M. (Eds), Lothagam. The Dawn of Humanity in Eastern Africa. Columbia University Press, New York. 261-328.

Werdelin, L., Lewis, M.E., 2001. A revision of the genus *Dinofelis* (Mammalia, Felidae). Zoological Journal of the Linnean Society 132, 147-258.

White, T.D., Asfaw, B., Beyene, Y., Haile-Selassie, Y., Lovejoy, C.O., Suwa, G., WoldeGabriel, G., 2009. *Ardipithecus ramidus* and the paleobiology of early hominids. Science 326, 75-85.

Wolpoff, M.H., Hawks, J., Senut, B., Pickford M., Ahern J., 2006. An ape or *the* ape: Is the Toumaï cranium TM 266 a hominid? PaleoAnthropology 2006, 36-50.

Wolpoff, M.H., Senut, B., Hawks, J., 2002. *Sahelanthropus* or '*Sahelpithecus*'? Nature 419, 581-582.

725 Wood, B., Boyle, E.K., 2016. Hominin taxic diversity: Fact or fantasy? Yearbook of Physical
726 Anthropology 159, 37-78.
727 Wood, B., Harrison, T., 2011. The evolutionary context of the first hominins. Nature 470, 347-
728 352.
729 Zollikofer, C.P.E., Ponce de León, M.S., Lieberman, D.E., Guy, F., Pilbeam, D., Likius, A.,
730 Mackaye, H.T., Vignaud, P., Brunet, M., 2005. Virtual cranial reconstruction of *Sahelanthropus*
731 *tchadensis*. Nature 434,755-759.
732

Table 1

Measurements of TM 266-01-063 (*S. tchadensis*) compared with BAR 1002'00 and BAR 1003'00 (both *O. tugenensis*) and with samples representing australopiths (*Australopithecus* and *Paranthropus*), modern humans (*H. sapiens*) and extant great apes (*Pan*, *Gorilla*, *Pongo*).

Variable	TM 266-01-63	BAR 1002'00	BAR 1003'00	Australopiths	*H. sapiens*	*Pan*	*Gorilla*	*Pongo*
Sub-trochanteric m-l diam. (mm)	31.6	25.7	27.3	29.5±4.9 23.5-38.9 (*n*=16)	32.5±2.4 27.4-38.3 (*n*=94)	27.6±2.2 23.5-34.0 (*n*=63)	38.6±4.6 29.3-45.9 (*n*=57)	23.4±4.2 19.3-30.1 (*n*=5)
Sub-trochanteric a-p diam. (mm)	25.3	20.4	22.0	22.2±4.0 16.9-29.6 (*n*=16)	24.1±2.5 18.7-30.8 (*n*=94)	23.4±1.6 20.5-27.8 (*n*=63)	32.5±4.1 24.7-39.3 (*n*=57)	19.3±1.8 16.6-21.0 (*n*=5)
Platymeric index (%)	80.1	79.4	80.6	74.6±3.7 66.4-81.5 (*n*=16)	74.3±6.6 60.6-88.9 (*n*=94)	85.3±5.8 71.1-102.4 (*n*=63)	84.3±5.1 76.5-101.3 (*n*=57)	83.3±8.8 69.6-91.9 (*n*=5)
Midshaft m-l diam. (mm)	28.3 [a]	25.5	26.3	24.7±2.4 21.9-27.8 (*n*=4)	26.0±1.9 21.1-31.1 (*n*=94)	25.7±2.2 21.4-29.2 (*n*=21)	41.3±3.9 32.8-46.6 (*n*=10)	22.0±3.9 17.9-27.9 (*n*=5)

Midshaft a-p diam. (mm)	26.2 [a]	20.8	21.3	22.9±2.0 21.0-25.0 (*n*=3)	27.0±2.7 21.7-33.5 (*n*=94)	24.5±2.3 21.4-30.1 (*n*=21)	33.6±2.7 26.9-36.2 (*n*=10)	19.2±2.5 16.1-23.1 (*n*=5)
Pilastric index (%)	92.6	81.6	81.0	93.1 89.9-95.9 (*n*=3)	104.1±9.3 88.3-128.0 (*n*=94)	95.5±6.8 83.3-109.6 (*n*=21)	81.6±4.3 73.8-88.0 (*n*=10)	87.5±6.2 79.6-94.5 (*n*=5)
Neck-shaft angle (°)	>135 [b]	124	-	119.3±4.7 112.5-125 (*n*=11)	127.4±4.1 113.3-136.3 (*n*=96)	123.1±5.1 109.3-133.3 (*n*=66)	118.9±5.1 106.0-129.0 (*n*=83)	134.0±5.2 127.3-145.1 (*n*=18)

For each comparative sample we provide the mean ± s.d., range, and sample size (*n*). Abbreviations: m-l = mediolateral; a-p = anteroposterior.

[a] Measured at the point of maximum anteroposterior curvature as seen in medial and lateral views (SOM Fig. S2).

[b] See SOM Fig. S1.

Caption to figures

Figure 1. The partial femur TM 266-01-063 from Toros-Menalla, Chad, in anterior (a), posterior (b), medial (c), and lateral (d) views. Scale bar = 2 cm.

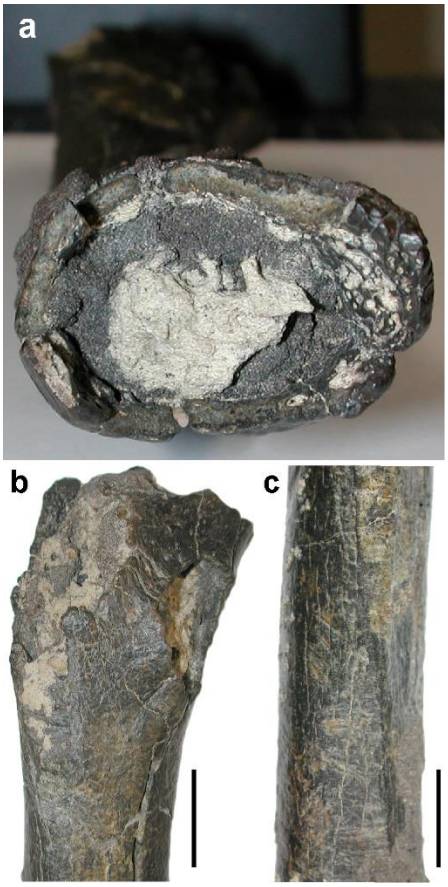

Figure 2. Details of TM 266-01-063. a) The naturally-broken, sediment-filled and slightly anteroposteriorly compressed distal end seen from below (anterior surface to the bottom; medial surface to the right). b) Posterior view of the proximal end (medial surface to the right). c) Posterolateral view of the midshaft region (medial surface to the right). Scale bar = 2 cm.

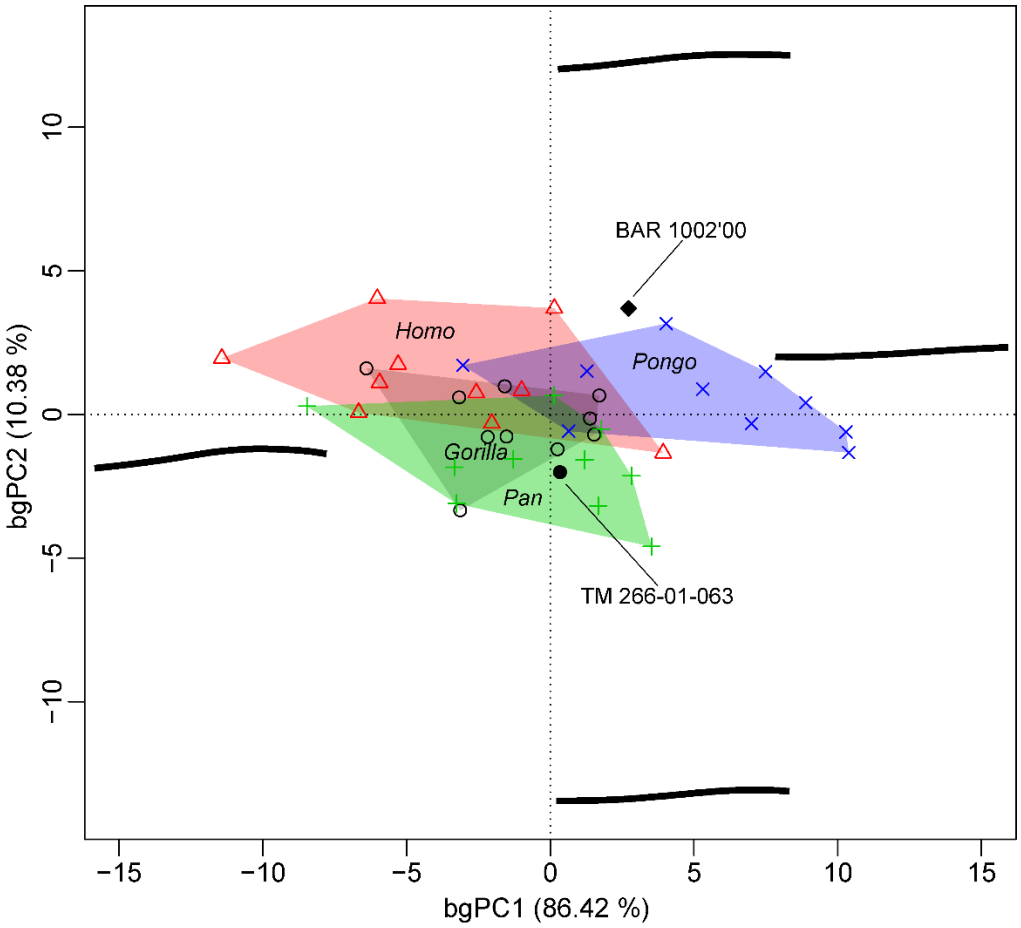

Figure 3. Between-group principal component analysis (bgPCA) of the Procrustes shape coordinates of the anterior femoral shaft curvature in TM 266-01-063, BAR 1002'00 (*Orrorin*) and four (µ)XCT-based subsamples representing *Homo sapiens* (*Homo* in the pink space) *Pan*, *Gorilla* and *Pongo*.

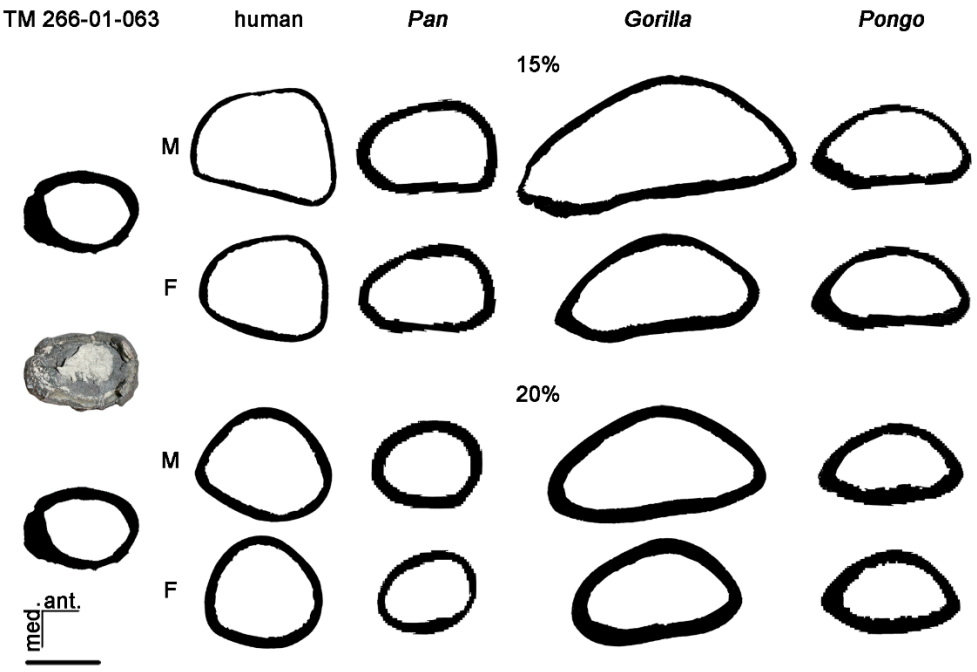

Figure 4. Virtual extraction of the cortical shell by manual delimitation of the endosteal and periosteal contours of the naturally broken and slightly anteroposteriorly compressed distal section of TM 266-01-63 (cf. Fig. 2a) and of (µ)CT-based virtual cross sections extracted at 15% (upper) and 20% (lower) of the biomechanical length in a female (F) and a male (M) femur representing *Homo sapiens*, *Pan*, *Gorilla* and *Pongo*. Scale bar = 2 cm.

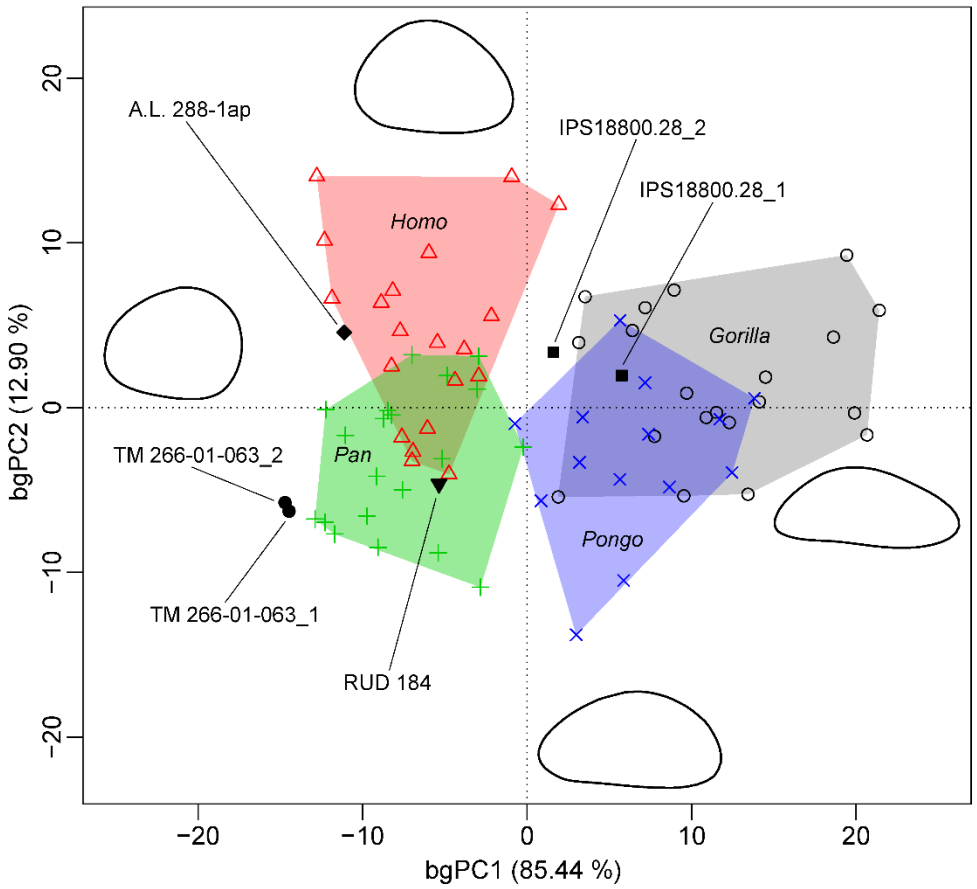

768

769 **Figure 5.** Between-group principal component analysis (bgPCA) of the Procrustes shape
770 coordinates of the cross-sectional contour of the distal femoral shaft in TM 266-01-063 (ca. 15%
771 of the estimated biomechanical length), A.L. 288-1ap (*Australopithecus afarensis*, ca. 20%),
772 IPS18800.28 (*Hispanopithecus laietanus*, ca. 17% [IPS18800.28_1] and ca. 20%
773 [IPS18800.28_2]), RUD 184 (*Rudapithecus hungaricus*, ca. 20%), and in four (μ)XCT-based
774 subsamples representing *Homo sapiens* (*Homo* in the pink space) *Pan*, *Gorilla* and *Pongo* (both
775 15% and 20% cross-sectional contours). TM 266-01-063 is represented by two reconstructed
776 outlines approximating its most likely original shape (TM 266-01-0631_1 and TM 266-01-063_2;
777 SOM Fig. 4).

778

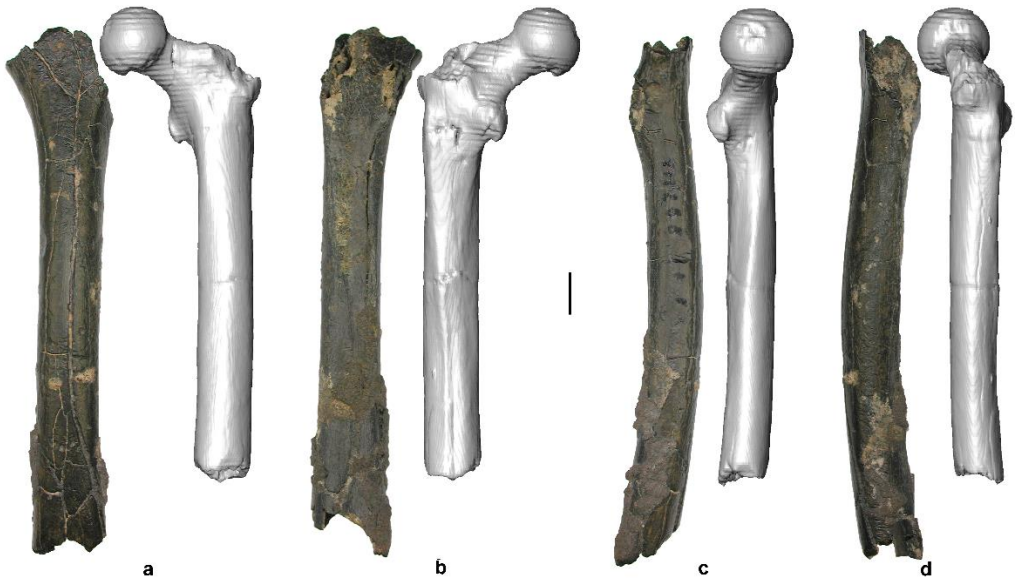

Figure 6. The partial femur TM 266-01-063 (left) in anterior (a), posterior (b), medial (c), and lateral (d) views compared to the CT-based reconstruction of BAR 1002'00 (Puymerail, 2011, 2017, based on a record kindly made available by B. Senut and M. Pickford). Technical characteristics of the CT-record are detailed in Galik et al. (2004); for additional 3D projections of BAR 1002'00, see also Kuperavage et al. (2018). Scale bar = 2 cm.

Supplementary Online Material (SOM)

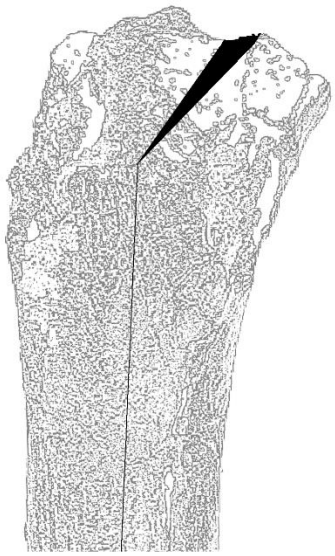

Figure S1. Sketch of the proximal preserved end of TM 266-01-063 in posterior view showing the estimation of the neck-shaft angle as defined by the long axis of the preserved shaft and the axis through the midpoint of the preserved base of the neck (cf. Köhler et al., 2002). The angle, ranging between 138° and 146°, was measured by ImageJ (Schneider et al., 2012) on different images of TM 266-01-063 in posterior view (the conservative measure of >135° is provided in Table 1).

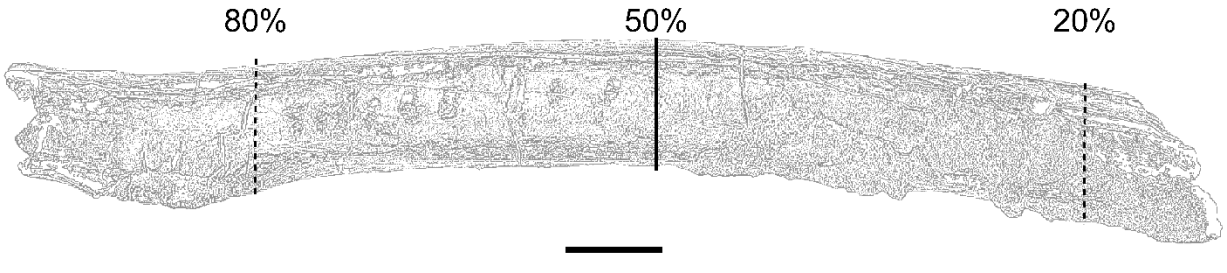

Figure S2. Sketch of TM 266-01-063 in medial view showing the approximate position of the cross sections at 80%, 50% and 20% for the assessment of the biomechanical length. The 80% section has been defined ca. 1 cm below the distal edge of the lesser trochanter, and the section at

50% (midshaft) at the point of maximum anteroposterior flexion of the shaft in medial and lateral views (Ruff et al., 1999; Ruff, 2000, 2002; Puymerail et al., 2012). Scale bar = 2 cm.

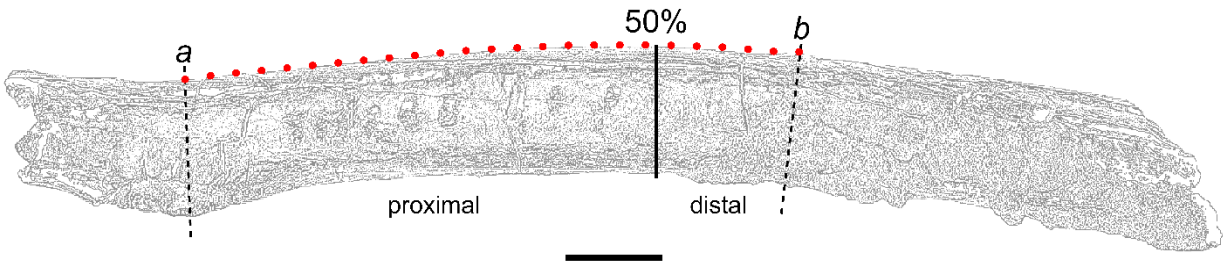

Figure S3. Sketch of TM 266-01-063 in medial view showing the protocol followed for assessing the degree of anteroposterior curvature of the femoral shaft. Using the TpsDig2 software (Rohlf, 2005), a total of 25 equidistant semilandmarks were digitized along the anterior outline between the point projected from the middle of the lesser trochanter (*a*) and ca. 40% of the biomechanical length (*b*). Scale bar = 2 cm.

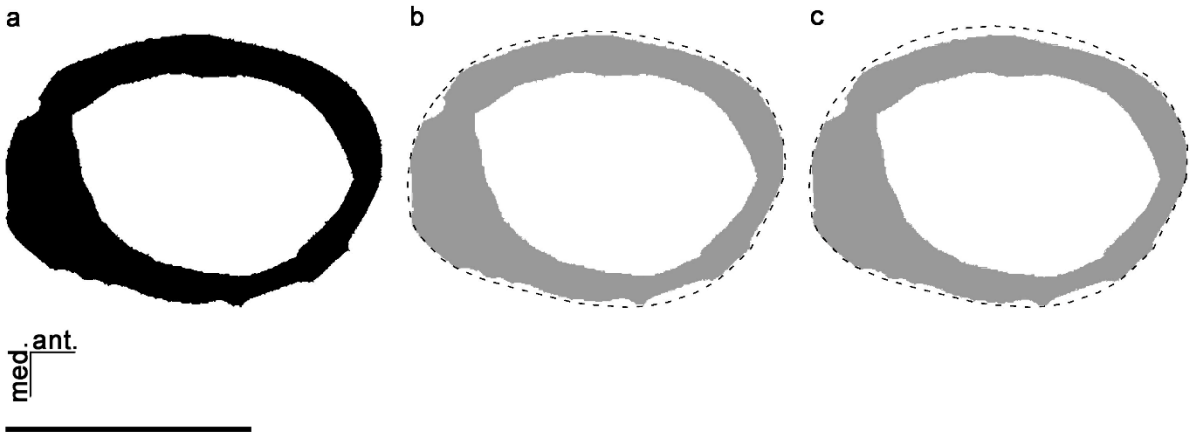

Figure S4. Sketch of the naturally-broken and slightly anteroposteriorly compressed distal end of TM 266-01-063 seen from below following delimitation of its cortical shell (a) and two corrected outlines, both used in the GM-based comparative analysis, generated to approximate its original outer contour in two ways (b, c). Using the TpsDig2 software (Rohlf, 2005), a total of 80

equidistant semilandmarks were digitized around the reconstructed outer outlines. Scale bar = 2 cm.

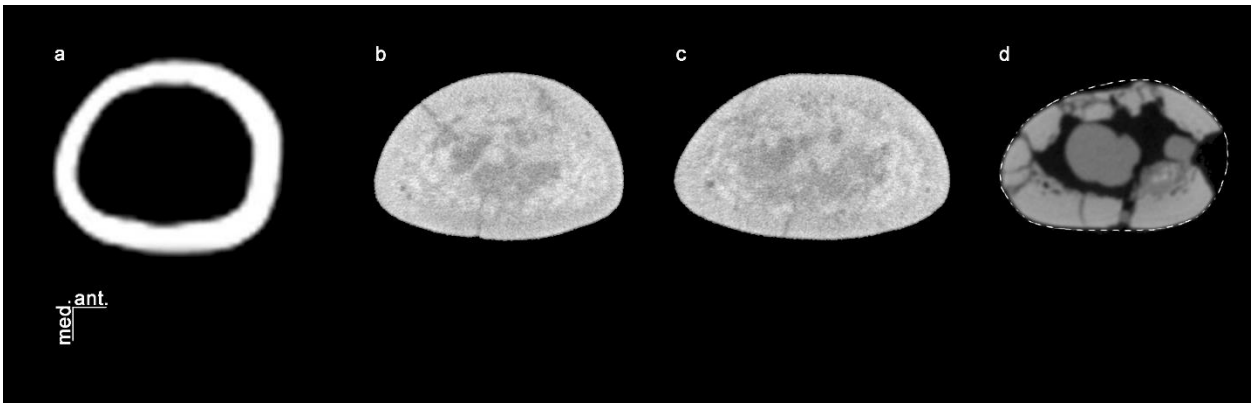

Figure S5. μXCT-based cross-sections of the distal femoral shaft. (a) The section at ca. 20% of the biomechanical length of the A.L. 288-1ap left femur (*Au. afarensis*; courtesy of C.B. Ruff and J.W. Kappelman). (b, c) The sections at ca. 17% (b) and ca. 20% (c) of the left femur IPS18800.28 (*Hispanopithecus*; courtesy of M. Pina and of the Institut Català de Paleontologia Miquel Crusafont); (d) The section at ca. 20% of the right femur RUD 184 (*Rudapithecus*; courtesy of D.R. Begun and R. Martin), whose external outline has been partially reconstructed to compensate for lateral damage and anteroposterior deformation. Images not to scale.

References

Köhler, M., Alba, D.M., Moyà Solà, S., MacLatchy, L., 2002. Taxonomic affinities of the Eppelsheim femur. American Journal of Physical Anthropology 119, 297-304.

Puymerail, L., Ruff, C.B., Bondioli, L., Widianto, H., Trinkaus, E., Macchiarelli, R., 2012. Structural analysis of the Kresna 11 *Homo erectus* femoral shaft (Sangiran, Java). Journal of Human Evolution 63, 741-749.

Rohlf, F.J., 2005. TpsDig2. TpsSeries. Department of Ecology and Evolution, SUNY, Stony Brook, New York.

Ruff, C.B., 2000. Body size, body shape, and long bone strength in modern humans. Journal of Human Evolution 38, 269-290.

Ruff, C.B., 2002. Long bone articular and diaphyseal structure in Old World monkeys and apes. I: Locomotor effects. American Journal of Physical Anthropology 119, 305-342.

Ruff, C.B., McHenry, H.M., Thackeray, J.F., 1999. Cross-sectional morphology of the SK 82 and 97 proximal femora. American Journal of Physical Anthropology 109, 509-521.

Schneider, C.A., Rasband, W.S., Eliceiri, K.W., 2012. NIH Image to ImageJ: 25 years of image analysis. Nature Methods 9, 671-675.